29B AFCRL-67-0076
9 JANUARY 1967 10
SPECIAL REPORTS, NO. 56

2 TERRESTRIAL SCIENCES LABORATORY 3 PROJECT 7628

1 **AIR FORCE CAMBRIDGE RESEARCH LABORATORIES**

L. G. HANSCOM FIELD, BEDFORD, MASSACHUSETTS 2

3 Terrestrial Multispectral Photography 6

6 J. F. CRONIN 9

This research was partially supported by
NASA DPR No. R22-13-012 ~~fund transfer~~ 29ACV

27 NASA ORDER

Distribution of this document is unlimited

20. its spec. Rept.-56 27

OFFICE OF AEROSPACE RESEARCH
United States Air Force

Abstract

Remote multispectral photographic sensing of the earth's surface may be a feasible means of identifying and discriminating between inorganic terrestrial materials differing in composition or physical characteristics. Simultaneous airborne and ground-based photographic and photometric studies of such sites as Mono Craters, California, indicate that within the range of the photographic spectrum (2900 Å to 14000 Å), the most promising region for the geologist and other earth scientists could be the wavelengths outside the visible spectrum.

Contents

1. INTRODUCTION 1

2. INSTRUMENTATION 2

   2.1 Aerial 2
   2.2 Ground 4
   2.3 Discussion 6

3. FIELD SITE STUDIES 6

   3.1 Mono Craters 8
   3.2 Pisgah Lava Field and Pisgah Crater 18
   3.3 South Cascade Glacier 19
   3.4 Coastal Areas 22

4. COMMENTS 22

ACKNOWLEDGMENTS 25

BIBLIOGRAPHY 25

Illustrations

Frontispiece. Mono Craters, California. Recent Volcanic Peaks of Rhyolitic Obsidian and Pumice facing 1

1. Multiband Camera, Camera Mount, and Control Panel in the AFCRL C-130 3

2. The AFCRL Pritchard Photometer 5

Illustrations

3.	Spectral Response of Pritchard Telephotometric System	5
4.	Aerial Photograph of Mono Craters, California	9
5.	Sketch Keyed to Terrain Features in Figure 4	10
6.	Aerial Photograph Showing Highly Reflective Pumice of Central Mono Craters	11
7.	Kodachrome Prints of Pumice and Lapilli Near Crater Peak	12
8.	Multiband Photographs of Crater Peak, Mono Craters, California	13
9.	Multiband Aerial Photographs of a Terminal (Talus) Slope of an Obsidian Flow, Photometric Site B, Mono Craters, California	15
10.	Multiband Photographs of Pumice and Lapilli, Photometric Site D, Central Mono Craters, California	16
11.	Kodachrome Prints of Thin-Section Photomicrographs of Desert Varnish Surface of Pahoehoe Lava, Pisgah Crater, California	20
12.	Spectral Reflectivities of Rock Types	21
13.	Aerial Photo of South Cascade Glacier	21
14.	Multiband Aerial Photographs of Rip Currents, Scripps Beach, La Jolla, California	23
15.	Multiband Aerial Photographs of Shore of Mono Lake, California	24
	APPENDIX A. Photometric Measurements of Field Sites, Mono Craters, California (16 Figures)	A1-A9

Table

1.	Photographic Flight Log	7

Mono Craters, California. Recent Volcanic Peaks of Rhyolitic Obsidian and Pumice (photographed at 6400 Å to 7000 Å)

Terrestrial Multispectral Photography

1. INTRODUCTION

The spectral range of electromagnetic sensing most familiar to geologists is the region of the visible wavelengths, between 4000 Å and 7000 Å. For more than a century, photochemical emulsions sensitive to this region of the spectrum have been used to capture reflected light and other radiant energy from terrestrial objects. For defining the size, shape, and spatial distributions of a feature, no other sensor can provide information as specific as that provided by photography.

A rather small group of earth scientists have for some time postulated that much more could be learned about the morphology, processes, and composition of the hydrosphere, lithosphere, and atmosphere by sensing simultaneously at several narrow bandwidths from 2900 Å to > 11000 Å, that is, throughout the photographic spectrum. Data obtained from the analysis of such narrowband multispectral photography would provide information not only about the interaction of electromagnetic radiation with the surface of the feature photographed but about the transmission and scattering properties of the intervening atmosphere. Interaction at the surface may result in reflection, polarization, scattering, or absorption, depending upon the microstructure of the surface and the atomic, molecular, or crystal structure of the material. Thus, variables that control the type, degree, and wavelength of the interaction include the chemical composition and optical properties of the material as well as its textural characteristics.

(Received for publication 10 January 1967)

The goal of our research on behalf of NASA has been to determine if the multispectral photographic technique might be feasible for identifying and discriminating between terrestrial materials differing in composition and/or physical characteristics. A request for us to evaluate the use of this technique in manned orbitors over terrestrial planetary bodies has not yet been acted upon but its desirability is being considered.

2. INSTRUMENTATION

2.1 Aerial

2.1.1 PHOTOGRAPHY

All aerial multiband photographs in this report were taken with the AFCRL 9-lens 70-mm aerial multiband camera. With such a camera, nine exposures can be made simultaneously, in nine different bandwidths of the photographic spectrum (Molineux, 1965). To date, the spectral range has been from 3850 Å to 9000 Å, each bandwidth determined by the lens/filter/film combination. Three exposures are made on each of three reels of film. Six of the nine exposures are on two reels of 250-ft 70-mm Plus X Aerographic film (Kodak type 5401); the other three are on one reel of 70-mm infrared Aerographic film (Kodak type 5424).

The camera body is a one-piece machined aluminum-alloy casting designed to fit directly into the camera mount. It has a stainless-steel focal-plane shutter with separate fixed apertures for each band. Speeds are 1/30, 1/60, or 1/120 sec. The camera operates through standard intervalometers and a standard image motion compensation system. The camera mount is a USAF ART-25 stabilized ring mount, but any mount (such as the A-28) that will accept the T-11 camera can be used.

For most of the flights we used nine Leitz C-106 f/2.4 lenses of 6-in. focal length; but at the lower altitudes and for the earlier flights we used Schneider f/2.8 Xenotar lenses. Filters were positioned between the lens element and held in place by snap rings. Filter sets were changed frequently in efforts to increase the peak transmission per band, to shift peak transmission to more desirable portions of the spectrum, to explore the less frequently used bandwidths, or to obtain better spectral matching with various soils, sediments, or rock surfaces.

Wratten filters, the only ones used until now, have proved less than desirable. In the field they rapidly became coated with dust or silt and were easily scratched; in the aircraft, over areas of high reflectivity such as deserts and glaciers, their transmission markedly deteriorated, and peak transmission shifted in wavelength. In the future only glass filters will be used.

During the mission, all camera operations were controlled from the camera control panel (Figure 1). Some of the panel controls are the power switch, IMC switch, V/H setting dials, manual tripping switch, intervalometer switch, and exposure counter.

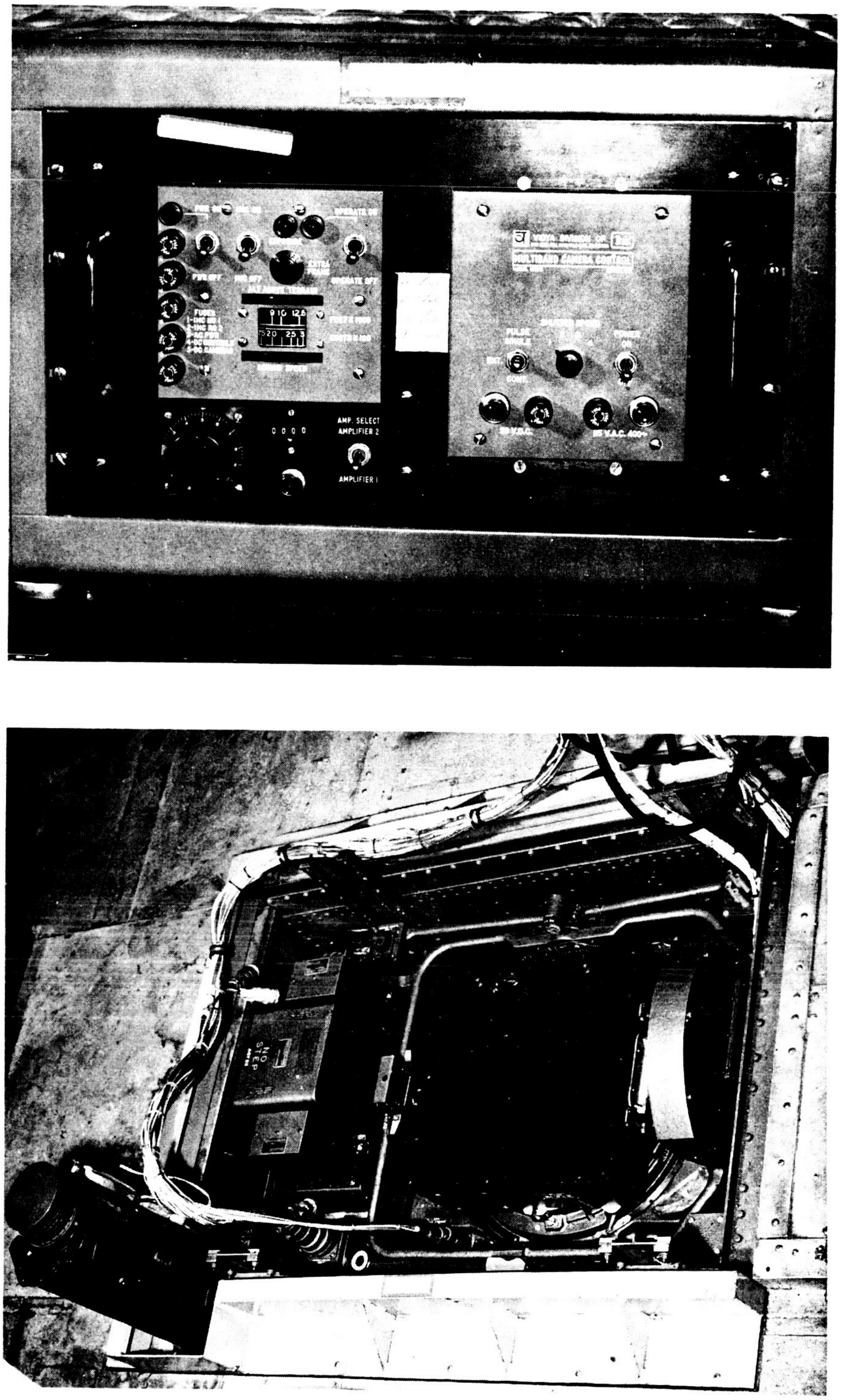

Figure 1. Multiband Camera, Camera Mount, and Control Panel in the AFCRL C-130

2.1.2 PHOTOMETRY

To date the only photometric measurements of the field sites have been those obtained on the ground from some distant observation point. The lack of a photometric capability in the aircraft of both NASA and USAF has been the most serious deficiency in our program. Until adequate photometry is possible from the air, evaluation or interpretation of an aerial multiband photograph is meaningless. Without such data as measurements of the irradiance of the sun and sky, together with that of the upwelling light from the whole terrain and the reflectance from the specific feature of interest within the field of view, demonstration of the feasibility of the aerial multiband technique is handicapped.

2.2 Ground

2.2.1 PHOTOGRAPHY

For all ground multiband photography we used a Graflex 4x5 Crown Graphic camera with a Schneider f/3.5 Xenotar lens of 135-mm focal length. To ensure greater uniformity of results we used the same 70-mm Aerographic Plus X and infrared films (Kodak types 5401 and 5424) in the Graflex camera as in the aerial 9-lens camera. This was made possible by means of a 70-mm Beattie-Coleman Transet adapter locked onto the back of the Graflex. In addition, the filters for both the ground and aerial cameras, as well as for the ground photometers, were all cut from the same sheet of filter material.

2.2.2. PHOTOMETRY

Two photometers were used in the field: a Pritchard photometer (Figure 2) with an S-11 photocathode photomultiplier tube, and a Gamma Scientific 700 Log Linear Photometer with an S-4 photomultiplier. The Pritchard was the workhorse instrument and provided all photometric data given in this report. It has a telescopic viewing system reflected from two mirrors, and a straight-through optical system for imaging directly on the photocathode of the photomultiplier tube. The photometer is therefore equally sensitive to light of any polarization. The objective lens has an adjustable focus. Between the aperture mirror and the photomultiplier there are two 6-position rotating turrets mounted one behind the other. These turrets contain the neutral-density filters and polarizing filters. An external filter holder was added so that filter combinations could be changed rapidly, and an MgO holder was mounted before the objective so that the sun's irradiance could be measured indirectly.

All photometry discussed in this report was limited to the range from 3800 Å to 7000 Å. Figure 3 is a typical response plot of the AFCRL Pritchard with the S-11 photomultiplier, as measured at AFCRL on a Zeiss monochromator and compared with a 2100°K blackbody reference.

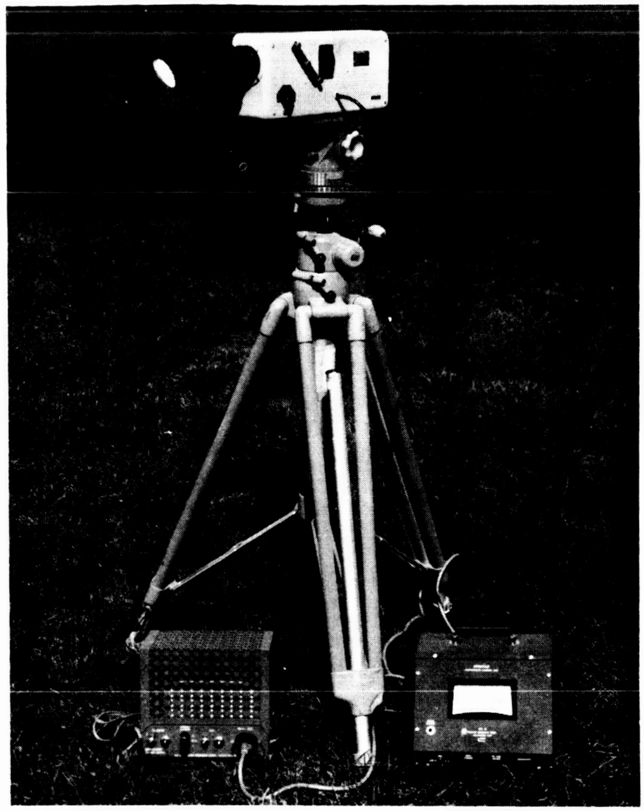

Figure 2. The AFCRL Pritchard Photometer

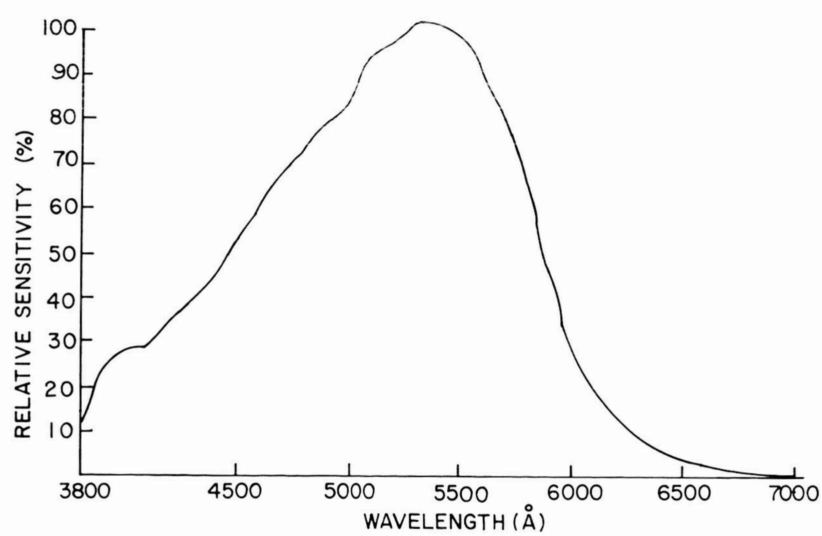

Figure 3. Spectral Response of Pritchard Telephotometric System (2100° K blackbody reference)

Our photometric studies are scheduled to be extended into the near ultraviolet and near infrared. In preparation, all glass in the Pritchard is being replaced by quartz; the S-11 photocathode is being replaced by an EMI photomultiplier tube with an S-20 photocathode in a quartz envelope. The spectral range of our Pritchard will be from 2900 Å to 8500 Å.

2.3 Discussion

The extreme limits of the photographic spectrum on Earth or of Earth from an orbital altitude are decisively restricted to 2900 Å and 14000 Å by a singular factor at each end of the spectrum.

At ultraviolet wavelengths, absorption of solar radiation by the ozone of Earth's atmosphere causes near-total extinction of the amount of solar energy radiating toward Earth's surface. (At the sun's zenith in midlatitudes, for example, the intensity of radiation on Earth at 2898 Å is only one millionth that at 3142 Å.) At the longer wavelengths, the limit of the photographic spectrum is determined by the photographic film. Various cyanine dyes can be adsorbed by the silver halide on the gelatin emulsion to extend the sensitivity of the film to almost 12500 Å but there are as yet no dyes that can sensitize farther into the infrared. The strong absorption of infrared radiation by the water in the gelatin of the film imposes a final upper limit at about 14000 Å.

3. FIELD SITE STUDIES

The field sites chosen for this study were, with one exception, nominated by a combined group of geologists from NASA, the U.S. Geological Survey, the Terrestrial Sciences Laboratory of the Air Force Cambridge Research Laboratories, and other similar institutions. The U.S. Geological Survey made the final selection. Early goals had been considered in terms of lunar analogs, and volcanic sites such as Pisgah Crater and Mono Craters became the initial areas for testing techniques. Mono Craters turned out to be an excellent choice for our purposes.

In addition to sites favored by NASA, AFCRL was interested in some that might be particularly suitable for both photographic and spectral photometric sensing. As a result, we have experimented with our techniques on the ground or from an aircraft, or both, at sedimentary areas in Arizona and Utah, playas in Death Valley, beaches in Puerto Rico, in the Apennine Mountains and over Mt. Vesuvius, and in Sardinia, Libya, and Nova Scotia. Since most of these efforts were carried out during the last six months, the data could not be processed in time to be included in this preliminary report, which deals with the locations listed in Table 1.

Table 1. Photographic Flight Log

Place	Date	Local Time	Altitude (ft)	Å (Lens) Bandwidth/Peak	Comments
Scripps Beach	21 April 1965	1630-1705	2500	(1) 3800-4900/4200 (2) 4500-5000/4600 (3) 5000-5400/5200 (4) 5500-5900/5600 (5) 5850-6350/6000 (6) 6550-7000/6800+ (7) 7250-8780/ – (8) 7800-8780/ – (9) 8400-8780/ –	No infrared film – magazine malfunction
Pisgah Crater	23 April 1965	0917-0919 0950-1016 1039-1059 1416-1428 1437-1458	11000 7000 2400 13000 7000	Same as above	No infrared film – destroyed in processing
Mono Craters	4 & 5 June 1965	(4) 0826-0909 (5) 0834-0933	7500 2500 & 9500	Same as above	
Cascade Glacier	23 Sept 1965	1330-1400	10000	(1) 3850/5000/4300 (2) 4300-5600/4950 *(3) 5150-6050/5520 (4) 5850-7000/6250+ *(5) 5150-6050/5520 (6) 6450-7000/7000 (7) 6850-8780/8780 (8) No data (9) 7400-8780/8780	* Lenses 3 and 5 were fitted with horizontal and vertical Polaroid type HN-38 linear polarizers, respectively
Mono Craters	9 Aug 1966	1241-1403 1515-1539	7500 14000	(1) 3850-4500/4200 (2) 4400-5250/4700 (3) 5050-5700/5250 *(4) 5500-6250/5725 *(5) 5300-6250/5725 (6) 6150/7000/ – (7) 7000/8780/ – (8) 7550-8780/ – (9) 7850-8780/ –	* Lenses 4 and 5 were fitted with horizontal and vertical Polaroid type HN-38 linear polarizers, respectively

Bands 1 to 6 inclusive, Aerographic Plus X Film, Kodak Type 5401
Bands 7 to 9 inclusive, Aerographic Infrared Film, Kodak Type 5424

3.1 Mono Craters

Mono Craters, in Mono County, California (Figures 4 and 5), lies at the foot of the escarpment of the Sierra Nevada. A region of intense volcanic activity during recent geologic time, it consists of a series of protrusions, domes, and craters from which have erupted intermittent rhyolitic obsidian flows and explosive ejections of rhyolitic ash, lapilli, and pumice. The uniformity of composition and extreme variability of texture, together with the relatively fresh, unweathered, unaltered nature of the materials in this area made it one of the more fortunate NASA selections for our particular kind of photographic and photometric study.

Of the four Mono Craters sites that AFCRL chose for a combined multispectral photographic and photometric analysis (Figure 4), the pair A and B are on the terminal slopes of the flows (coulees), and the pair C and D are within an area heavily mantled by the fall of pumice and lapilli. Figure 6, which is a conventional aerial photograph of this ejection mantle, illustrates the high reflectivity of the mantle materials (see also the frontispiece). The thickest deposition is centered upon Crater Peak and its immediate vicinity (see Figure 7). The boundaries of the mantle are rather poorly defined. There has been no attempt made to map the mantle at a scale appropriate to sensor analysis.

In Figure 8, a set of ground-level multiband photographs of the highest peak of Mono Craters, the intensely reflective rhyolitic volcanic pumice and lapilli blanketing the crestal regions appears to increase in reflectivity with increase in wavelength, up to 7000 Å. Between 6550 Å and 9000 Å, however, there is a marked decrease in reflectivity, which is most obvious when it is noted that the grass in the foreground (Views C and D) does not show a corresponding decrease; for all prints in this report, gamma was determined visually.

Spectrophotometric analysis of rhyolite has confirmed the increase in reflectivity from 4000 Å to 7000 Å, but as yet there are no data available in the near infrared (>7000 Å) to either confirm or dispute this reversal in intensity of fragmental rhyolite between 6550 Å and 9000 Å. Reliable spectrophotometric analysis of lithic materials throughout the photographic spectrum is scarce indeed, and analyses based on the grain size, shape, rounding, and vesicularity of unconsolidated materials or on the packing and linearity of grains in consolidated materials are nonexistent. J. B. Adams of Jet Propulsion Laboratory has been studying igneous rocks for some time, and is expected to be publishing some results of interest in this field. The U. S. Geological Survey, as well as AFCRL, will soon initiate its own investigations.

Figure 4. Aerial Photograph of Mono Craters, California (A, B, C, D: sites of photometric analysis; O: point of observation)

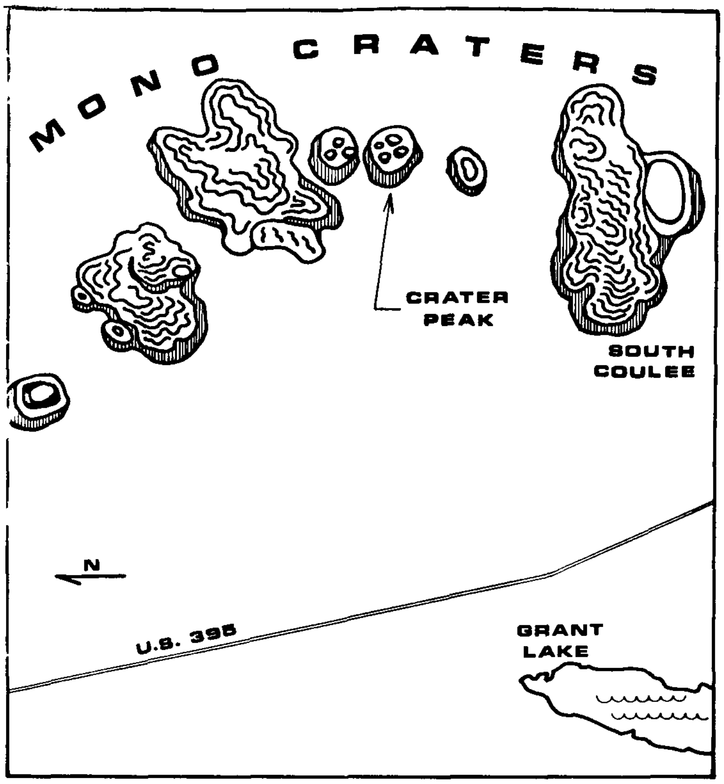

Figure 5. Sketch Keyed to Terrain Features in Figure 4

The fundamental parameters of importance in studies of this type can be categorized under the following headings.

I. Atmospheric Optical Characteristics

A. The angle of incidence of the solar flux

B. The wavelength or spectral distribution of sky radiation and the solar flux

C. The polarization of sky radiation and the solar flux

D. Atmospheric attenuation
   1. Coefficient of Rayleigh scattering
   2. Coefficient of aerosol scattering
   3. Coefficient of ozone absorption
   4. Extinction coefficient (visibility or visual range)
   5. Rayleigh optical thickness from sea level to the altitude of observation, and from the altitude of observation to infinity (to space)
   6. Extinction optical thickness from sea level to the altitude of observation, and from the altitude of observation to infinity

Figure 6. Aerial Photograph Showing Highly Reflective Pumice of Central Mono Craters (plus X film, no filter)

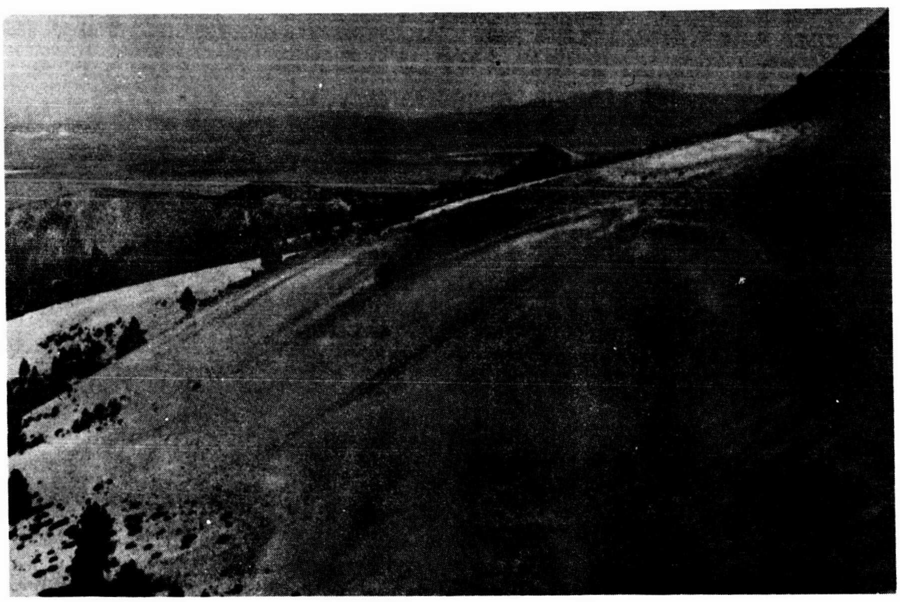

Figure 7. Kodachrome Prints of Pumice and Lapilli Near Crater Peak

II. Terrestrial Surface Characteristics

A. Optical properties
   1. Atomic, molecular, or crystal structure (chemical composition)

B. Surface geometry
   1. Microrelief
      a) Size of particles or fragments (consolidated or unconsolidated)
      b) Shape
      c) Roundness
      d) Linearity (packing)

C. Surface moisture and surface temperature

D. Weathering or oxidation (coating)

III. Meteorologic Environment

A. Wind velocity and direction

B. Humidity

C. Shelter temperature

D. Cloud cover (type and amount)

IV. Elevation

Our intention is not to actually measure all these components in the field, but to use Elterman's (AFCRL) model of a turbid atmosphere. Elterman's model is characterized by aerosol- and ozone-attenuating components in addition to the molecular or Rayleigh attenuation components of the U. S. Standard Atmosphere. It allows for such exploratory exercises as this study, provided adequate photometric measurements are made. Without aerial photometry all interpretations are subject to considerable doubt or modification.

Figure 9 is a set of three low-altitude multiband photographs, with a sketch, of a talus slope of one of the obsidian flows at Mono Craters; this shows our photometric site B (see also Figure 4). It is readily apparent that maximum reflectance from the talus slope is at the shorter wavelengths (the upper left photograph). Again, in Figure 10, our photometric site D, maximum contrast is at the shorter wavelengths. Note particularly the upper left quadrant of the two photographs of this figure.

Whether there is sufficient radiation at near-ultraviolet wavelengths to penetrate the atmosphere twice (from the sun down through the atmosphere to the ground and then back up to the aircraft), is doubted by many workers. The current consensus is that at near-ultraviolet wavelengths the apparent contrast between a feature and its background is so diminished and attenuated by the atmosphere that it is imperceptible to a sensor. We here at AFCRL do not agree.

Figures 9 and 10 illustrate that greater detail is produced at the shorter wavelengths. At present we are not certain about the explanation, but the responsible factors must include (1) the angle of incidence of solar radiation, (2) the spectral reflectance characteristics of the feature, (3) the spectral distribution of sky and solar radiation at the moment of photography, and (4) the elevation of the feature.

Direct solar ultraviolet intensity increases with increasing elevation above sea level as the radiation passes through thinner layers of the atmosphere, with less absorption. Since site D is 8500 ft above sea level, Figure 10 should therefore show a slight increase in solar ultraviolet radiation.

The photographs in Figure 10 were taken within 15 min of solar zenith (apparent noon). At that time, when the path of radiation through the atmosphere is shortest, the solar ultraviolet radiation is at its daily maximum. Notwithstanding the corresponding loss of scattered ultraviolet radiation from the sky with the increase in elevation (the lower, more turbid, part of the atmosphere being responsible for most of the ultraviolet scattering), the net increase in solar ultraviolet radiation during this particular photographic flight must have been great enough – perhaps unusually so – to have provided maximum contrast detail at the shorter wavelengths. Spectral data taken during the flight at ground level is being processed, as is that obtained for Figure 9. Using these data and Elterman's atmospheric attenuation model as a basis for comparison we may be able to arrive at a more convincing interpretation of these examples.

Returning to Figure 9, here again the reflectance at the shorter wavelengths (A) is apparently more intense than that at the longer wavelengths. It is probable that the angle of incidence of solar radiation and the spectral distribution of sky radiation are as significant in this instance as in Figure 10. The predominant factors, however, are the solar elevation and the direction and degree of slope of the talus.

The slope of the talus is approximately 35°, dipping due west. The solar elevation on this date and at this hour of the morning was 38°. The angle of incidence of the solar rays (grazing angle) was thus approximately 3°. At low solar elevations on a clear day the sky component of short-wavelength radiation may be as much as or more than the solar component. Irradiation of the slope at the shorter wavelengths was therefore primarily from the sky, due to Rayleigh or aerosol scattering. Since the intensity of Rayleigh scattering is proportional to $1/\lambda^4$, at 4200 Å [spectral peak in (A)], Rayleigh scattering alone is 16 times that at 8400 Å [spectral peak in (C)]. The long shadows within the landslide area of the slope demonstrate that there is some irradiance of the slope by the sun, but most of this irradiance must be reflected at a low angle above the outwash plain in the foreground. The geometry of the sun's elevation and azimuth and the degree and direction of the slope is therefore the prime factor in the greater reflectivity of the feature at the shorter wavelengths. Hence, if an orbiting spacecraft or an aircraft is required to photograph a feature or target on the earth at low solar elevations, results may be improved by using restricted bandwidths in the near-ultraviolet region.

To determine the pertinent factors and ascertain their significance, we photometrically measured all four sites for six hours during three days of a four-day period in September 1966. The results are presented as Appendix A, consisting of 16 graphs in which reflectance values in milliwatts per square centimeter are plotted against time and the angle θ between the path of the sun's incident rays on the feature of interest and the line of sight of the photometer.

Meteorological conditions on the first and third days were almost identical. The maximum temperature was about 75°F, there was a slight haze in the morning (to 1100 PDT), winds gusted to 8 or 10 mph from midmorning through the rest of the day, and the sky was cloudless. On the middle day of the three, 10 September, there was a heavier haze and very thin cirrus clouds until 1230 PDT, with 2/10 alto cumulus over the Sierra Nevada from 1300 hr on .

Our preliminary analyses of the data obtained on 8, 10, and 11 September 1966 indicate that at ground level:

1. Photography at short wavelengths is optimum under conditions of maximum θ values.
2. Photography at long wavelengths is optimum under conditions of minimum θ values.
3. Polarized reflectance (and contrast) is, as expected, maximum at $\theta \cong 90°$.

After thorough analysis of the field photometric data for the four sites at Mono Craters, including laboratory analysis to define the textural characteristics and optical properties of the various materials collected at each site, we expect to present a more comprehensive evaluation than is possible in this interim report. For a full and scientifically meaningful interpretation, however, we are looking forward to the acquisition of data recorded on an airborne photometric system.

3.2 Pisgah Lava Field and Pisgah Crater

The Pisgah lava flows and the Pisgah Crater are in the Mohave Desert not far from Barstow, California. All flows are of olivine basalt and of relatively recent origin in geologic time. The flows vary in texture from aa to pahoehoe, that is, from a rough, blocky, slaglike surface to a smooth, ropy surface. Although we had been furnished the necessary geologic information and base maps by the U. S. Geological Survey, several considerations forced us to abandon our sensor field studies at Pisgah.

Alluvium, and particularly windblown shifting sand, partly covers the flows and so obscures the true surface from the camera lens that experimental flights are impossible to duplicate from one month to the next, or even, in some seasons, from day to day. More significantly, this windblown sand and silt is in part directly responsible for a readily apparent gloss or polish of exposed surfaces of certain lavas and clastics derived from these lavas. This "desert varnish" is most evident on the smoother lavas, the pahoehoe. The result is a surface coating (Figure 11), 10 to 100μ thick, usually insoluble, of iron or manganese oxide, which can quite effectively mask the inherent character of the rock from visual or photographic observation. A photograph of such a surface is simply a photograph of the coating only.

And finally, the one consideration that outweighs perhaps all others in selecting a site is the anticipated optical response of the site materials. Basic igneous rocks, of which the Pisgah olivine basalt is an example, have the lowest reflectivities, and of all the major rock types – metamorphic rocks not excepted – produce the least suggestion of a characteristic response in the visible spectrum. (See Figure 12.)

The Pisgah lava field was thus the least suitable of all the sites chosen. Understandably, no further work is planned here.

3.3 South Cascade Glacier

This small glacier (Figure 13) is in the northern Cascade Range, roughly 75 miles northeast of Seattle, Washington. It has been under intensive investigation by the U.S. Geological Survey since 1957. During late September of 1965, the USGS obtained multispectral photographs in flights over the glacier while Cronin and Molineux of AFCRL were making photometric measurements on the ice field. In such an environment, factors in the surface patterns include pools and channels of water on the surface of the ice, crevasses, air bubbles and cavities in the ice, and impurities such as sediment and dust in the ice and snow. Differences in texture and color can sometimes be exceedingly hard to distinguish because of reflectivity from the fields of ice, firn, and snow.

To date, the only multispectral photographic film we have received on South Cascade Glacier is third-generation copy. Its interpretation, analysis, and evaluation would not be worthwhile or valid since the subtle differences existing in the original have undoubtedly suffered degradation in the copying processes. A more extensive treatment of this data is therefore postponed until we have had an opportunity to examine the original material.

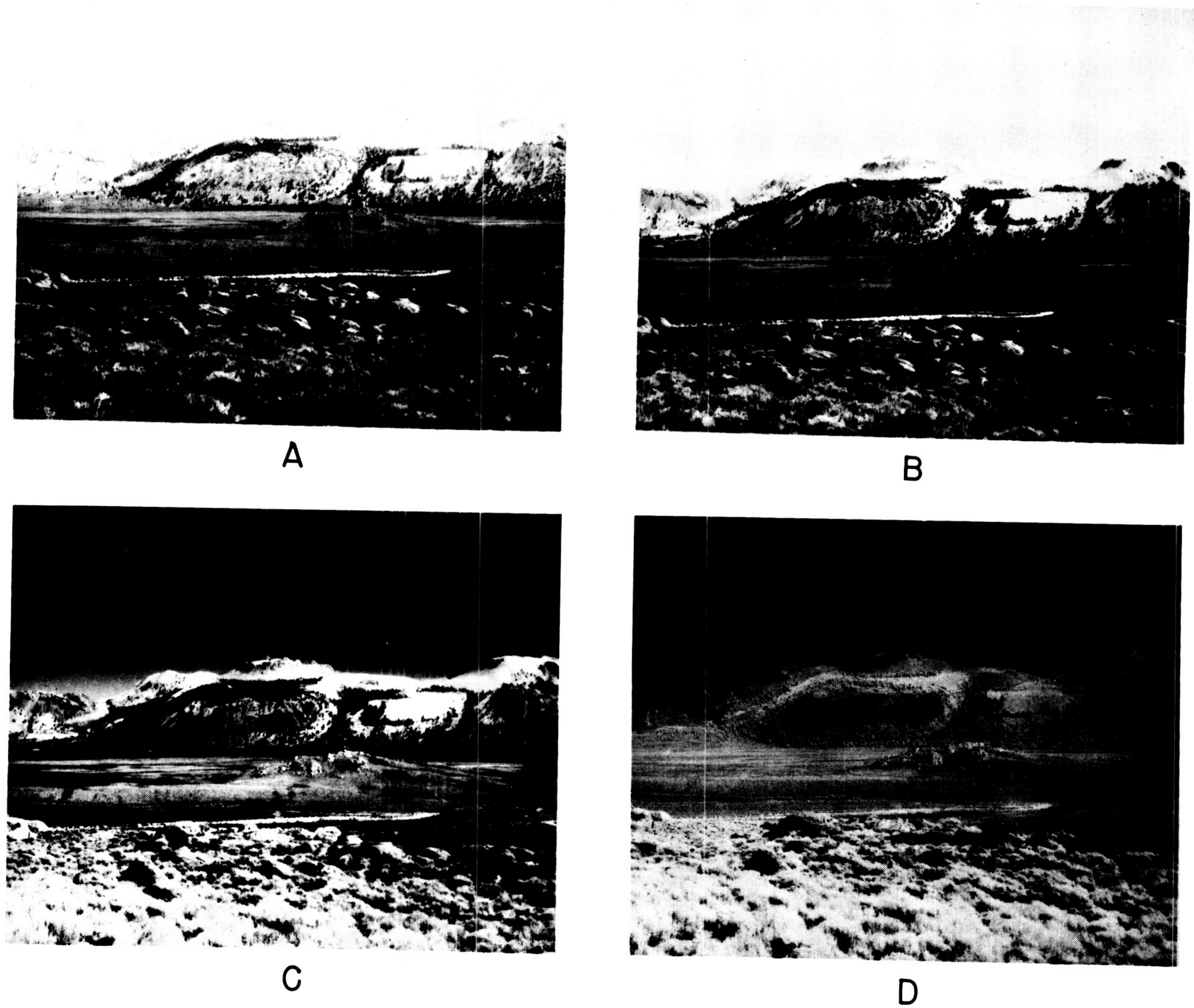

Figure 8. Multiband Photographs of Crater Peak, Mono Craters, California [photographic wavelength bands: (A) 3800 Å - 4900 Å; (B) 4400 Å - 5550 Å; (C) 6550 Å - 7000 Å; (D) 7250 Å - 9000 Å]

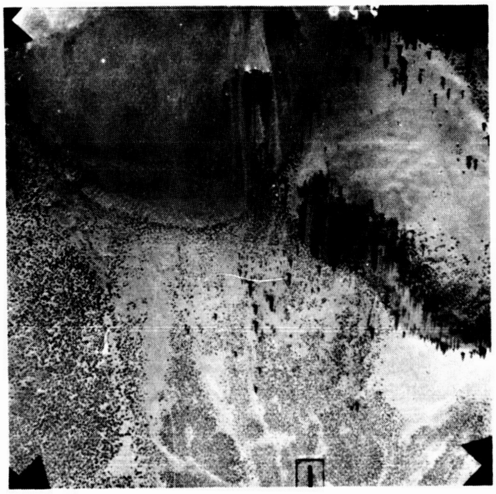

A

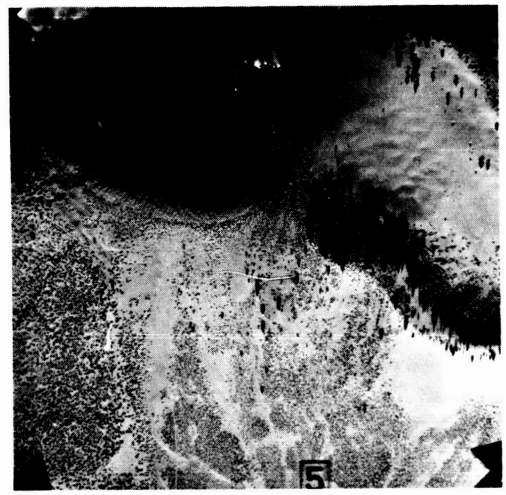

B

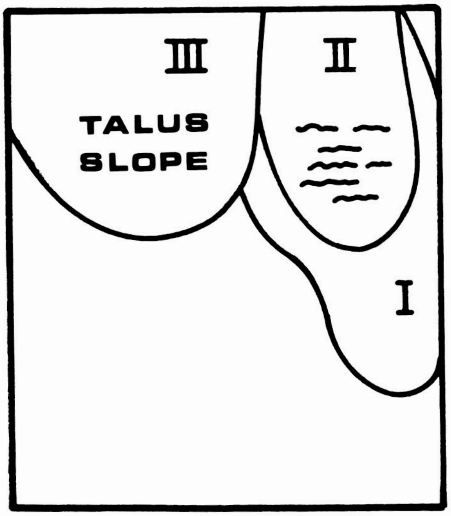

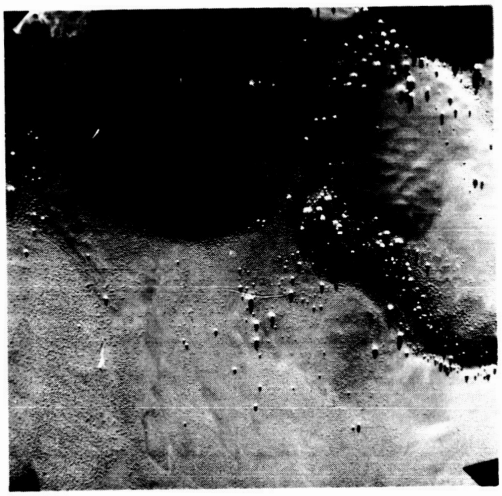

C

Figure 9. Multiband Aerial Photographs of a Terminal (Talus) Slope of an Obsidian Flow, Photometric Site B, Mono Craters, California [photographic wavelength bands: (A) 3800 Å - 4900 Å; (B) 5850 Å - 6350 Å; (C) 7250 Å - 9000 Å] [0915 hr, 5 June 1965; altitude: 2500 ft above terrain]

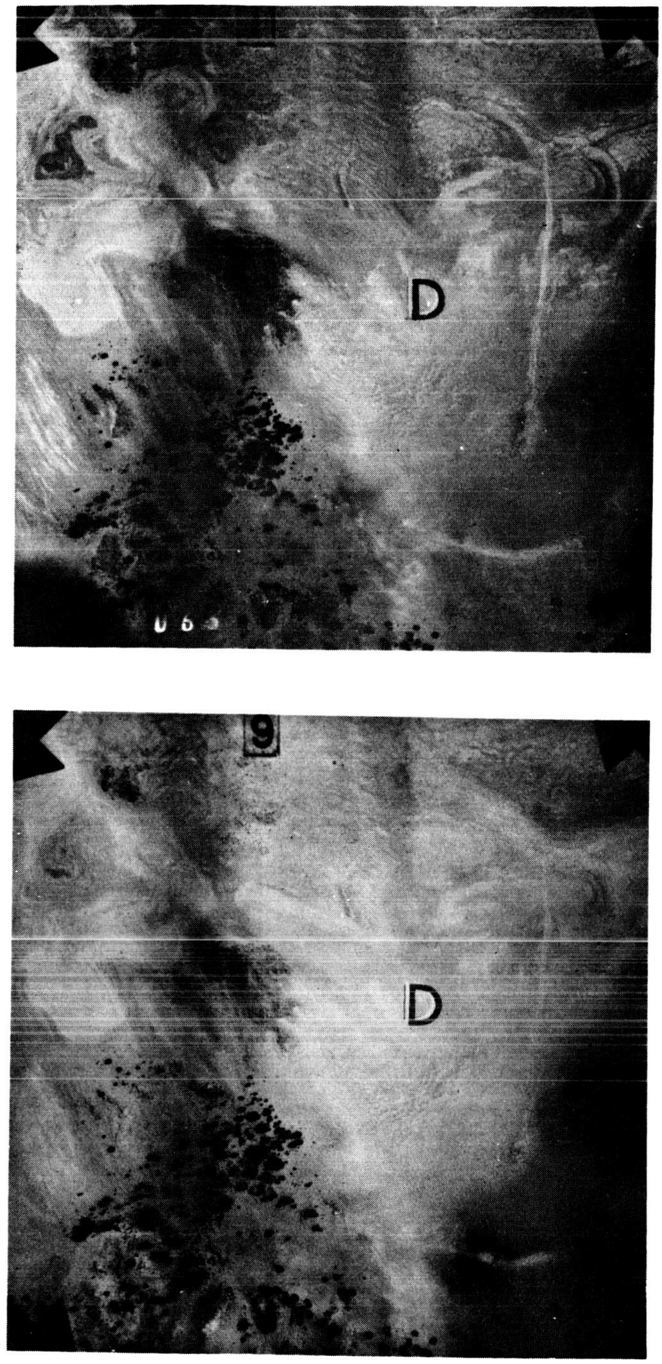

Figure 10. Multiband Photographs of Pumice and Lapilli, Photometric Site D, Central Mono Craters, California (photographic wavelength bands: upper, 3800 Å - 4900 Å; lower, 6550 Å - 7000 Å)

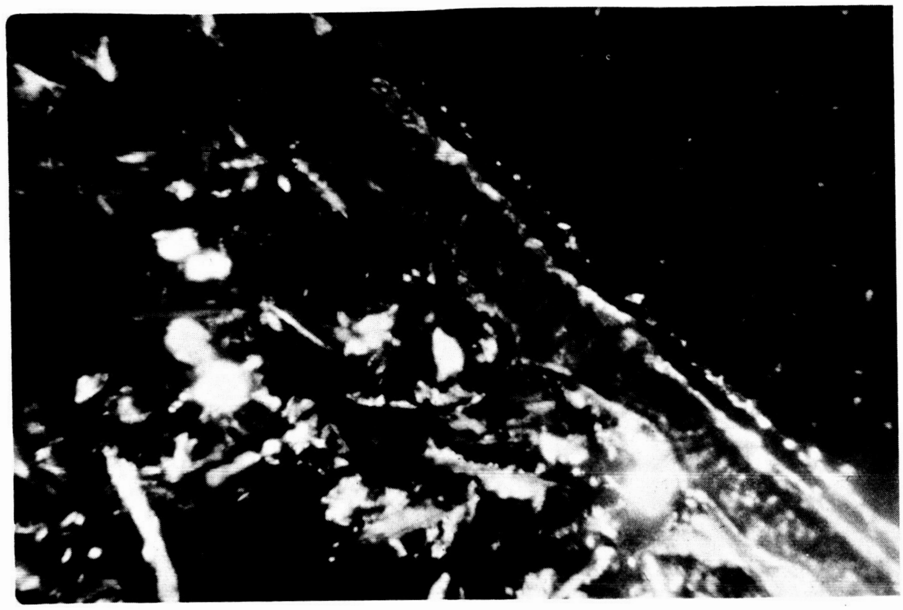

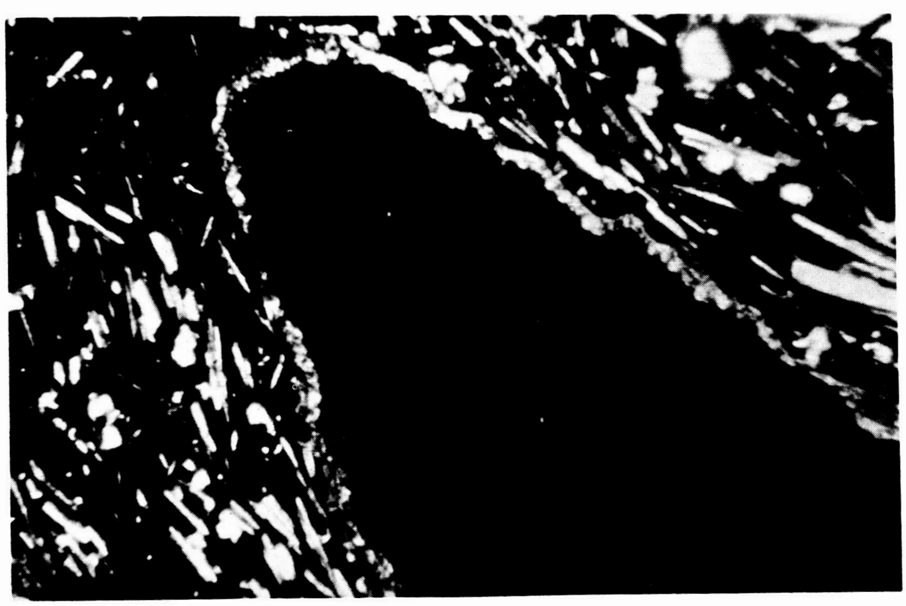

Figure 11. Kodachrome Prints of Thin-Section Photomicrographs of Desert Varnish Surface of Pahoehoe Lava, Pisgah Crater, California (lower view is of an exposed vesicle)

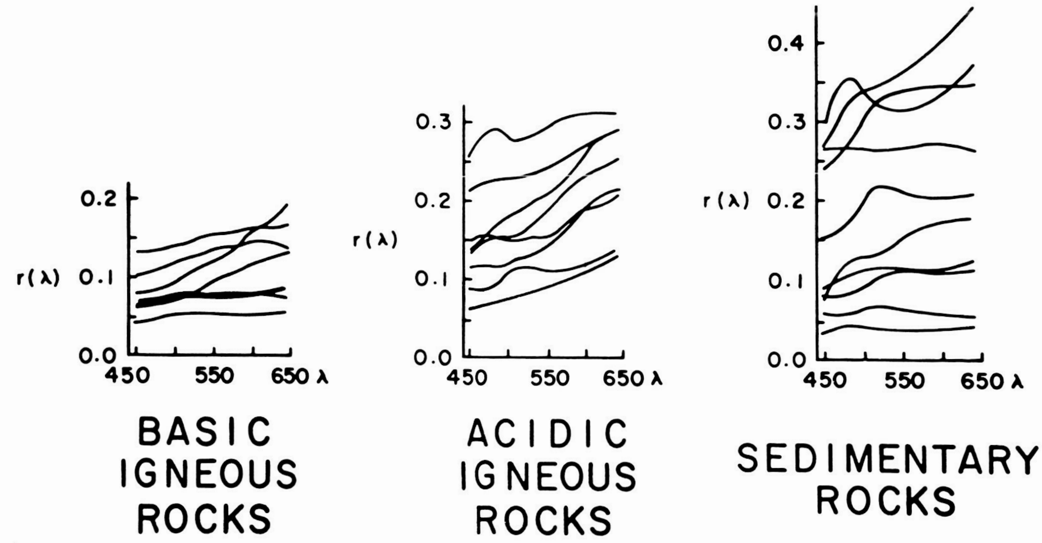

Figure 12. Spectral Reflectivities of Rock Types (after V. V. Sharonov)

Figure 13. Aerial Photo of South Cascade Glacier

3.4 Coastal Areas

It is known that fresh waters and coastal waters have their maximum transparency at 5000 Å to 6000 Å. In multiband photographs of a rip current (Figure 14) at Scripps Beach, La Jolla, California, the structure of the current is best revealed within this same spectral range – more specifically, at 5000 Å to 5400 Å. The bottom configuration of inland bodies of water such as the coastal strip of Mono Lake (Figure 15) at the mouth of Rush Creek is documented with maximum detail in the band from 5000 Å to 5400 Å.

Obviously, there are many processes that might best be studied at selected or restricted wavelengths. Those of civic importance include water discharge, water mass boundaries, erosion, coastal circulation, and the salt content of municipal, industrial, or irrigation waters. Those of military importance are outside the scope of this report.

4. COMMENTS

This investigation has not produced a new or revolutionary technique, but it has exposed possibilities of research that should be developed. Aircraft and field teams must be better instrumented to gather spectral photometric data. Wavelengths outside the visible region but within the photographic spectrum appear to be the most promising regions for earth science studies. The correlation of the spectral photometric characteristics of the feature, optical and attenuation characteristics of the atmosphere, and photographic bandwidth is of utmost importance. Polarimetric and goniophotometric studies are highly desirable. The lack of appropriate maps of adequate scale and content has been a particularly frustrating handicap at all the test sites. Fine-detailed geologic maps of lithologic units and subunits are needed – not just the usual maps of the exposures of consolidated materials but those of unconsolidated clastic and nonclastic sediments and, in some cases, of residual soils. Maps of gross variations in texture, composition, moisture content, and other characteristics of unconsolidated sediments are also vital. It is hoped that the current interest of the U. S. Geological Survey in some of these sites will spur early publication of the detailed information, reports, and maps that are prerequisite to any extensive aircraft program of sensor investigations.

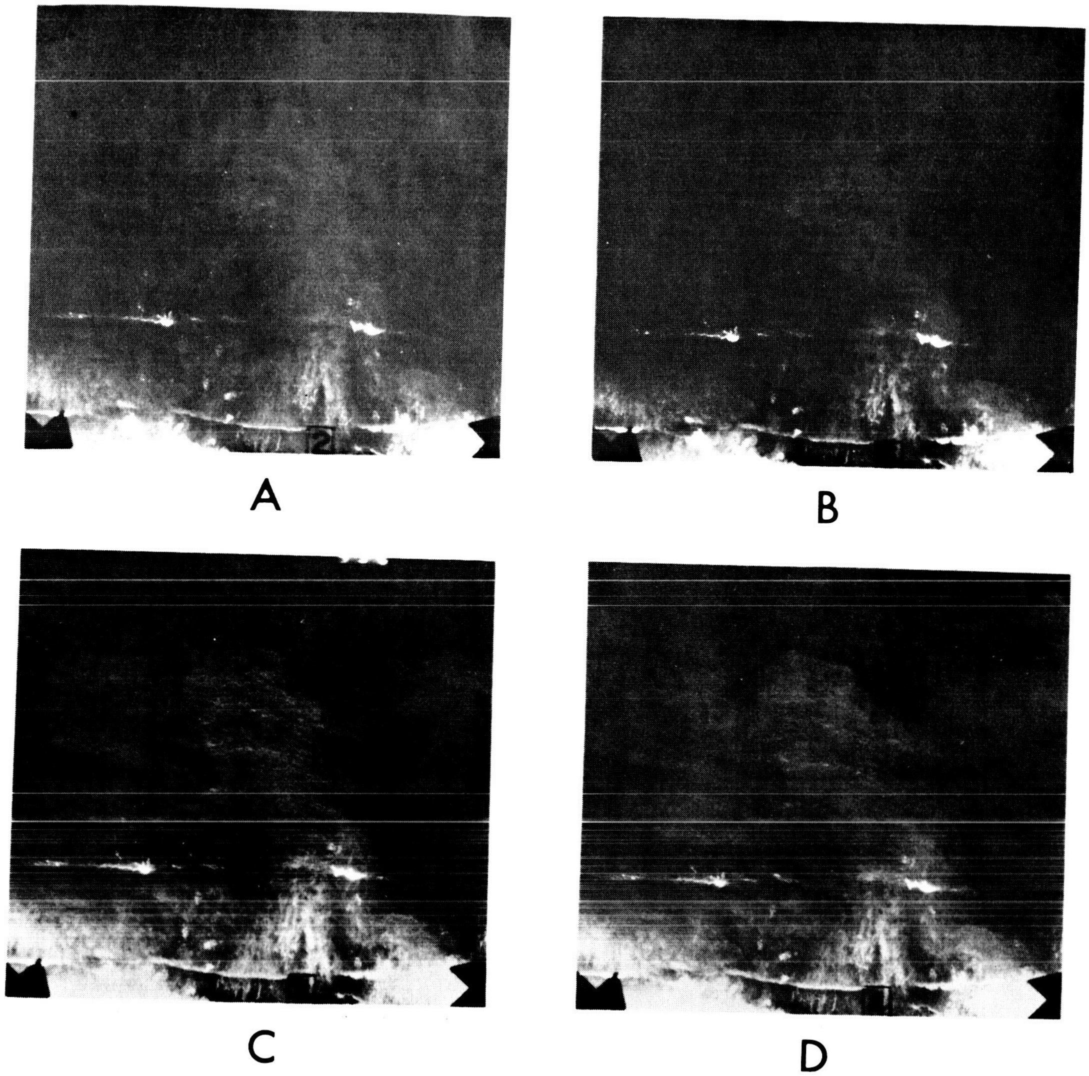

Figure 14. Multiband Aerial Photographs of Rip Currents, Scripps Beach, La Jolla, California (photographic wavelength bands: (A) 4500 Å - 5000 Å; (B) 5900 Å - 6300 Å; (C) 5000 Å - 5400 Å; (D) 5500 Å - 5900 Å) [1515 hr, 21 April 1965; altitude: 7000 ft above terrain]

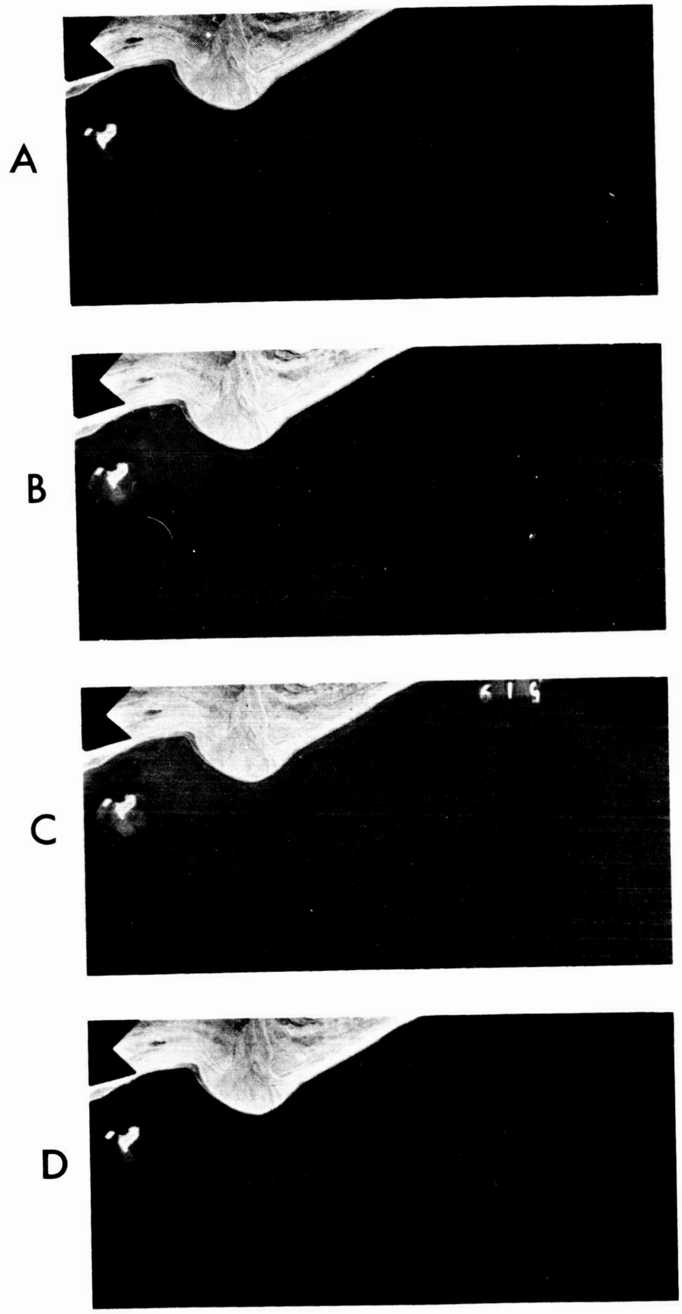

Figure 15. Multiband Aerial Photographs of Shore of Mono Lake, California (photographic wavelength bands: (A) 4500 Å - 5000 Å; (B) 5000 Å - 5400 Å; (C) 5500 Å - 5900 Å; (D) 5900 Å - 6300 Å) [0900 hr, 5 June 1965; altitude: 2500 ft above terrain]

Acknowledgments

Members of the AFCRL Terrestrial Sciences Laboratory contributing significantly to the work reported are Roland E. Hudson, Sgt, USAF, who was the aerial photographer, and Richard W. Dowling and Carlton E. Molineux, who cooperated in the laboratory and in the field.

We are most are most appreciative of the cooperation of the Houston Manned Spacecraft Center (NASA) personnel who assisted us during our joint aircraft program.

Special acknowledgment is given to personnel of the U. S. Geological Survey in Washington, D. C.; Menlo Park, California; and Seattle, Washington; for their valuable and encouraging assistance during the past two years of our association.

Critical review of the manuscript by Robert B. Toolin of the AFCRL Optical Physics Laboratory is acknowledged.

Bibliography

Clarke, G. L., and Denton, E. J. (1962), in Physical Oceanography (Vol. 1 in The Sea, M. M. Hill, Ed.), Interscience, N. Y., pp. 456-468.

Elterman, L. (1963), A Model of a Clear Standard Atmosphere for Attenuation in the Visible Region and Infrared Windows, AFCRL-63-675.

Fenn, Robert W. (1966), Correlation Between Atmospheric Backscattering and Meteorological Visual Range, AFCRL-66-549.

Bibliography

Gilbert, Charles M. (1938), Welded tuff in eastern California, Bull. Geol. Soc. Am. 49: 1829-1862.

Gilbert, Charles M. (1941), Late tertiary geology southeast of Mono Lake, California, Bull. Geol. Soc. Am. 52: 781-816.

Kistler, Ronald W. (1966), Geologic Map of the Mono Craters Quadrangle, Mono and Tuolumne Counties, California, U.S. Geol. Surv. Map GQ-462.

Mayo, E. ., Conant, L.C., and Chelikowsky, J.R. (1936), Southern extension of the Mono Craters, California, Am. J. Sci. 32: 81-97.

Molineux, Carlton E. (1965), Multiband spectral system for reconnaissance, Photogrammetric Engineering 31: 131-143.

Pakiser, L.C., Press, F., and Kane, M.F. (1960), Geophysical investigation of Mono Basin, California, Bull. Geol. Soc. Am. 71: 415-448.

Pakiser, L.C., Kane, M.F., and Jackson, W.H. (1964), Structural Geology and Volcanism of Owens Valley Region, California — a Geophysical Study, U.S. Geol. Surv. Prof. Paper 438.

Russell, Israel C. (1889) Quaternary history of Mono Valley, California, U.S. Geol. Surv. 8th Ann. Rpt, pp. 795-842.

Sharonov, V.V. (1956) Vestnik Leningradskogo Universiteta 11(No. 1): 155-167.

Smith, Robert L. (1960), Ash flows, Bull. Geol. Soc. Am. 71: 795-842.

Valley, Shea L., Scientific Editor, Handbook of Geophysics and Space Environments (1965), Air Force Cambridge Research Laboratories, Office of Aerospace Research, United States Air Force.

Williams, Howel (1932), The history and characters of volcanic domes, Univ. Calif. Publ. Geol. Sci. 21: 51-135.

Appendix A

Photometric Measurements of Field Sites, Mono Craters, California

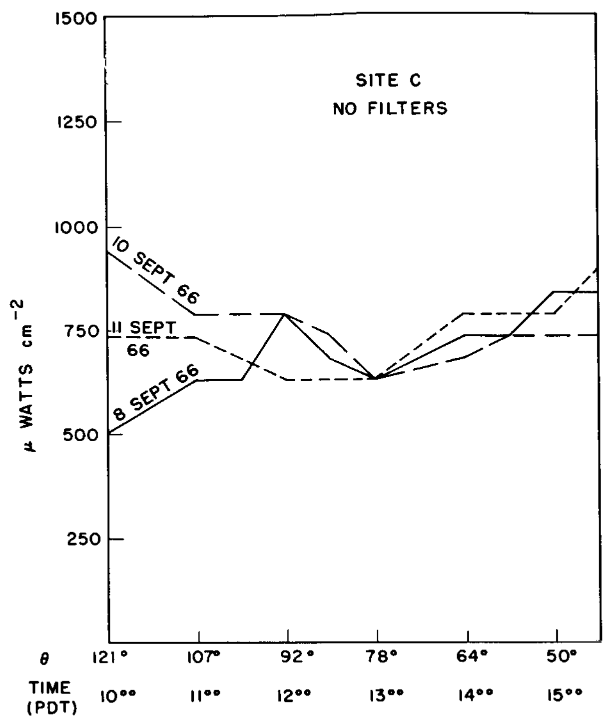
1500
1250
1000
750
500
250
SITE C
NO FILTERS
10 SEPT 66
11 SEPT 66
8 SEPT 66
μ WATTS cm^-2
θ
121°
107°
92°
78°
64°
50°
TIME (PDT)
10^00
11^00
12^00
13^00
14^00
15^00

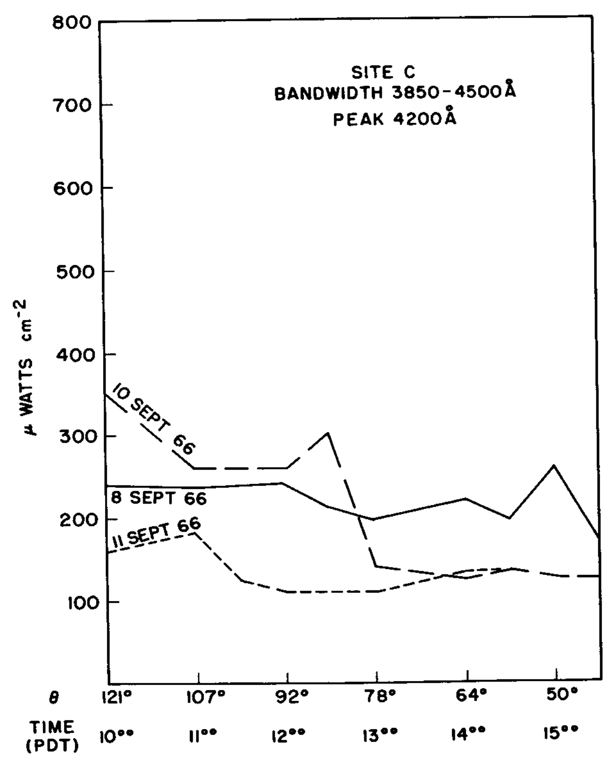
800
700
600
500
400
300
200
100
SITE C
BANDWIDTH 3850-4500Å
PEAK 4200Å
10 SEPT 66
8 SEPT 66
11 SEPT 66
μ WATTS cm^-2
θ
121°
107°
92°
78°
64°
50°
TIME (PDT)
10^00
11^00
12^00
13^00
14^00
15^00

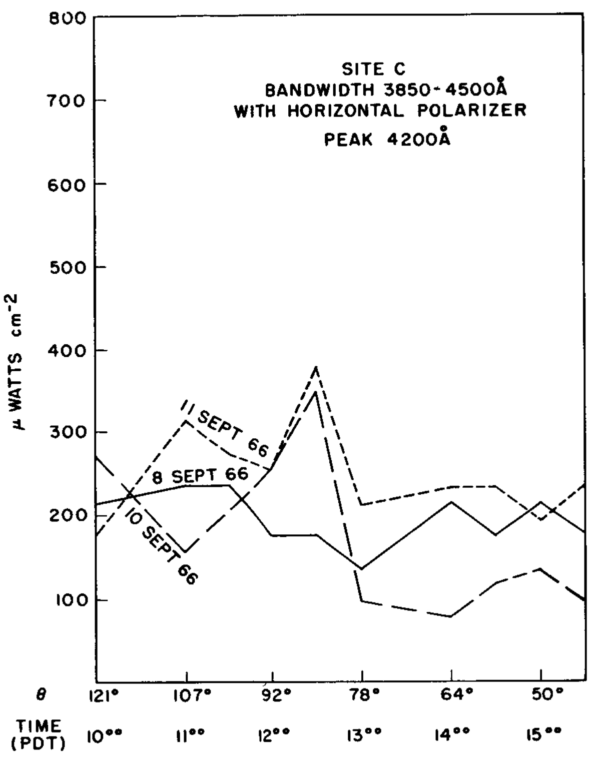
SITE C
BANDWIDTH 3850-4500Å
WITH HORIZONTAL POLARIZER
PEAK 4200Å
800
700
600
500
400
300
200
100
μ WATTS cm⁻²
11 SEPT 66
8 SEPT 66
10 SEPT 66
θ
121°
107°
92°
78°
64°
50°
TIME (PDT)
10⁰⁰
11⁰⁰
12⁰⁰
13⁰⁰
14⁰⁰
15⁰⁰

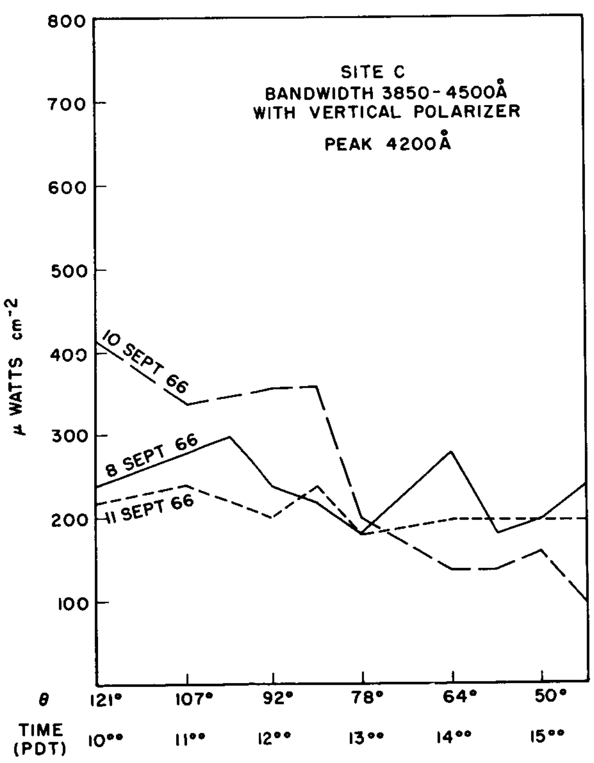
SITE C
BANDWIDTH 3850-4500Å
WITH VERTICAL POLARIZER
PEAK 4200Å
800
700
600
500
400
300
200
100
μ WATTS cm⁻²
10 SEPT 66
8 SEPT 66
11 SEPT 66
θ
121°
107°
92°
78°
64°
50°
TIME (PDT)
10⁰⁰
11⁰⁰
12⁰⁰
13⁰⁰
14⁰⁰
15⁰⁰

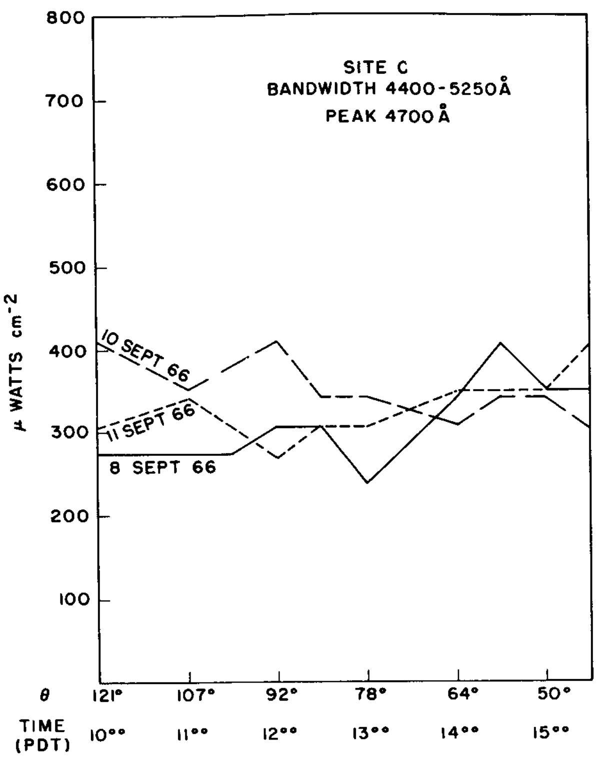
SITE C
BANDWIDTH 4400-5250Å
PEAK 4700Å
μ WATTS cm-2
10 SEPT 66
11 SEPT 66
8 SEPT 66
800
700
600
500
400
300
200
100
θ
121°
107°
92°
78°
64°
50°
TIME (PDT)
10⁰⁰
11⁰⁰
12⁰⁰
13⁰⁰
14⁰⁰
15⁰⁰

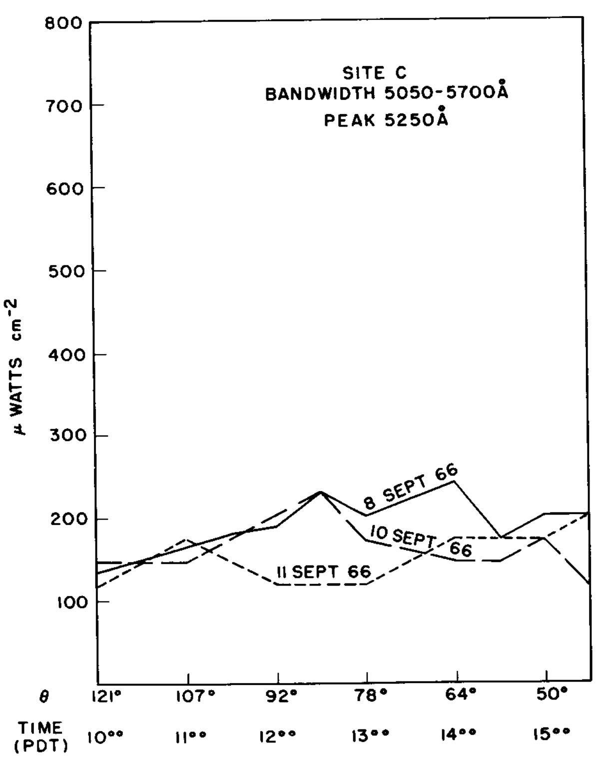
SITE C
BANDWIDTH 5050-5700Å
PEAK 5250Å
μ WATTS cm-2
8 SEPT 66
10 SEPT 66
11 SEPT 66
800
700
600
500
400
300
200
100
θ
121°
107°
92°
78°
64°
50°
TIME (PDT)
10⁰⁰
11⁰⁰
12⁰⁰
13⁰⁰
14⁰⁰
15⁰⁰

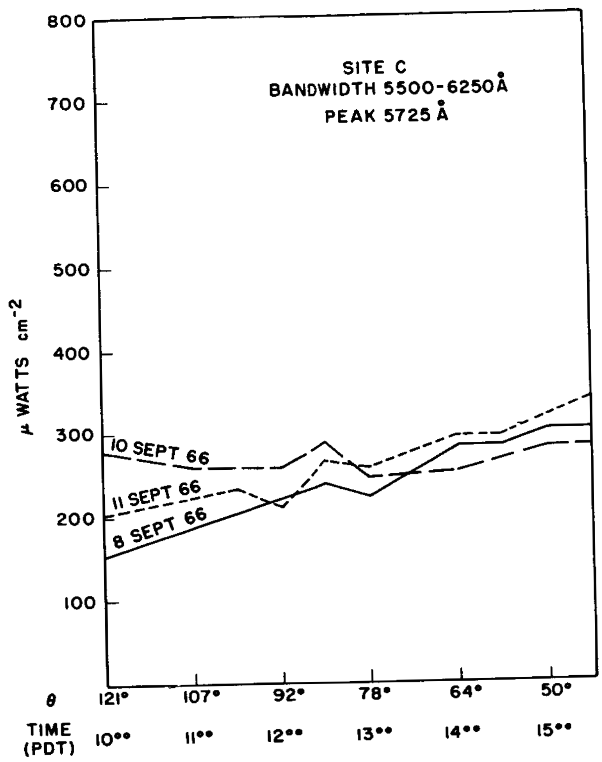
SITE C
BANDWIDTH 5500-6250Å
PEAK 5725 Å
μ WATTS cm⁻²
800
700
600
500
400
300
200
100
10 SEPT 66
11 SEPT 66
8 SEPT 66
θ
121°
107°
92°
78°
64°
50°
TIME (PDT)
10⁰⁰
11⁰⁰
12⁰⁰
13⁰⁰
14⁰⁰
15⁰⁰

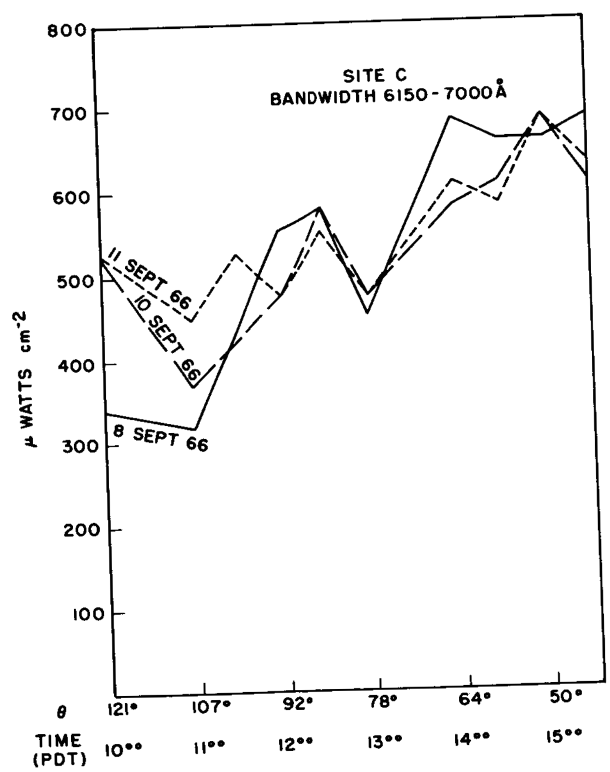
SITE C
BANDWIDTH 6150-7000Å
μ WATTS cm⁻²
800
700
600
500
400
300
200
100
11 SEPT 66
10 SEPT 66
8 SEPT 66
θ
121°
107°
92°
78°
64°
50°
TIME (PDT)
10⁰⁰
11⁰⁰
12⁰⁰
13⁰⁰
14⁰⁰
15⁰⁰

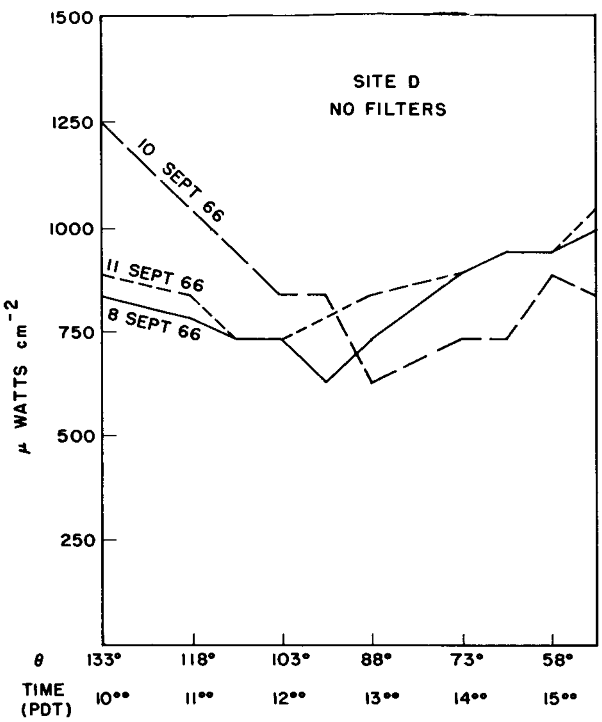
SITE D
NO FILTERS
1500
1250
1000
750
500
250
μ WATTS cm⁻²
10 SEPT 66
11 SEPT 66
8 SEPT 66
θ
133°
118°
103°
88°
73°
58°
TIME (PDT)
10⁰⁰
11⁰⁰
12⁰⁰
13⁰⁰
14⁰⁰
15⁰⁰

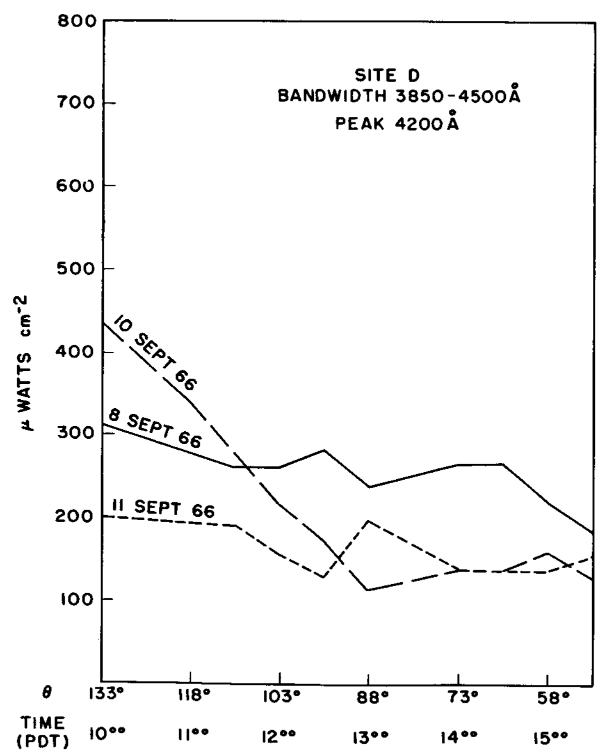
SITE D
BANDWIDTH 3850-4500Å
PEAK 4200Å
800
700
600
500
400
300
200
100
μ WATTS cm⁻²
10 SEPT 66
8 SEPT 66
11 SEPT 66
θ
133°
118°
103°
88°
73°
58°
TIME (PDT)
10⁰⁰
11⁰⁰
12⁰⁰
13⁰⁰
14⁰⁰
15⁰⁰

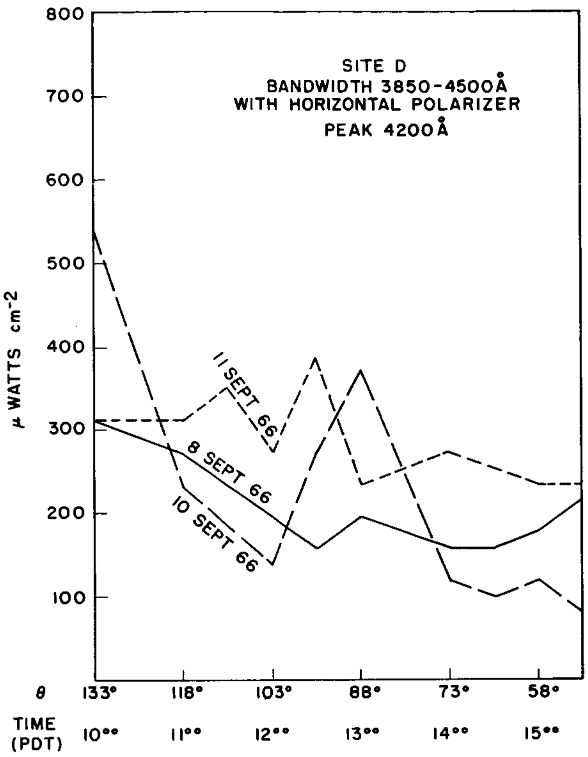
SITE D
BANDWIDTH 3850-4500Å
WITH HORIZONTAL POLARIZER
PEAK 4200Å
μ WATTS cm-2
800
700
600
500
400
300
200
100
11 SEPT 66
8 SEPT 66
10 SEPT 66
θ
133°
118°
103°
88°
73°
58°
TIME (PDT)
10:00
11:00
12:00
13:00
14:00
15:00

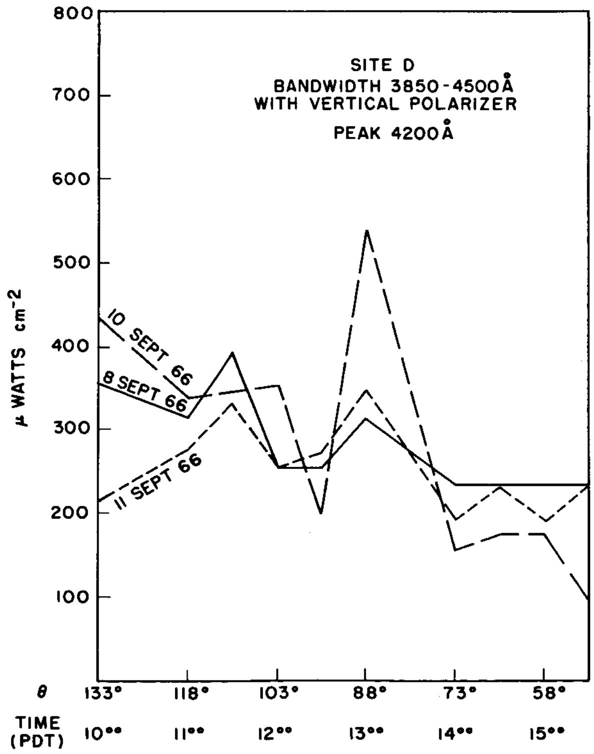
SITE D
BANDWIDTH 3850-4500Å
WITH VERTICAL POLARIZER
PEAK 4200Å
μ WATTS cm-2
800
700
600
500
400
300
200
100
10 SEPT 66
8 SEPT 66
11 SEPT 66
θ
133°
118°
103°
88°
73°
58°
TIME (PDT)
10:00
11:00
12:00
13:00
14:00
15:00

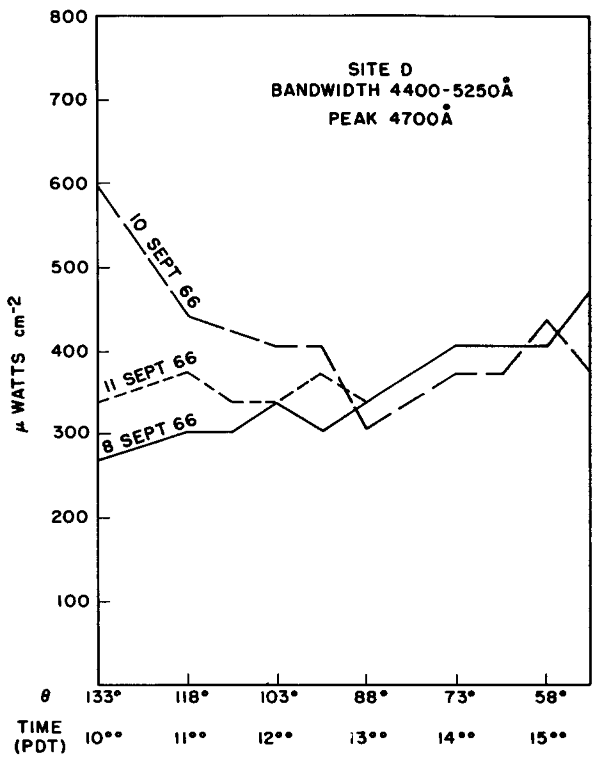
800
700
600
500
400
300
200
100
μ WATTS cm-2
SITE D
BANDWIDTH 4400-5250Å
PEAK 4700Å
10 SEPT 66
11 SEPT 66
8 SEPT 66
θ
133°
118°
103°
88°
73°
58°
TIME
(PDT)
10°°
11°°
12°°
13°°
14°°
15°°

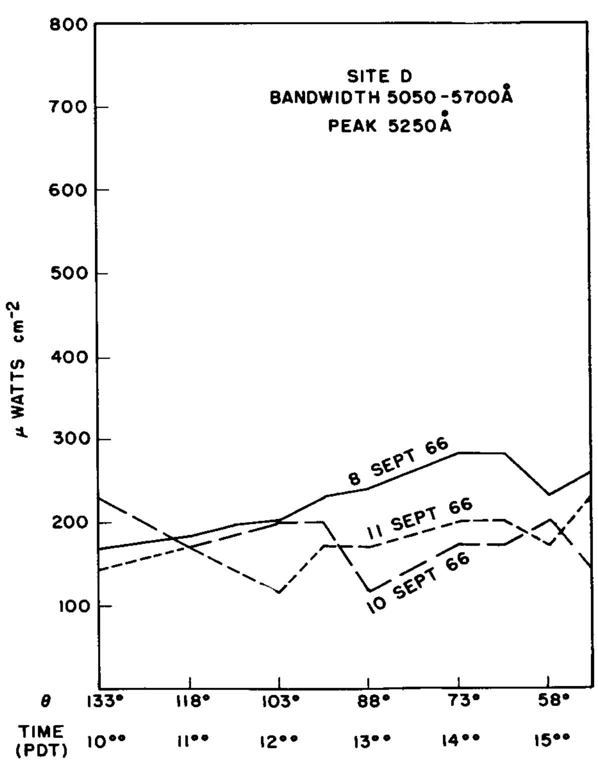
800
700
600
500
400
300
200
100
μ WATTS cm-2
SITE D
BANDWIDTH 5050-5700Å
PEAK 5250Å
8 SEPT 66
11 SEPT 66
10 SEPT 66
θ
133°
118°
103°
88°
73°
58°
TIME
(PDT)
10°°
11°°
12°°
13°°
14°°
15°°

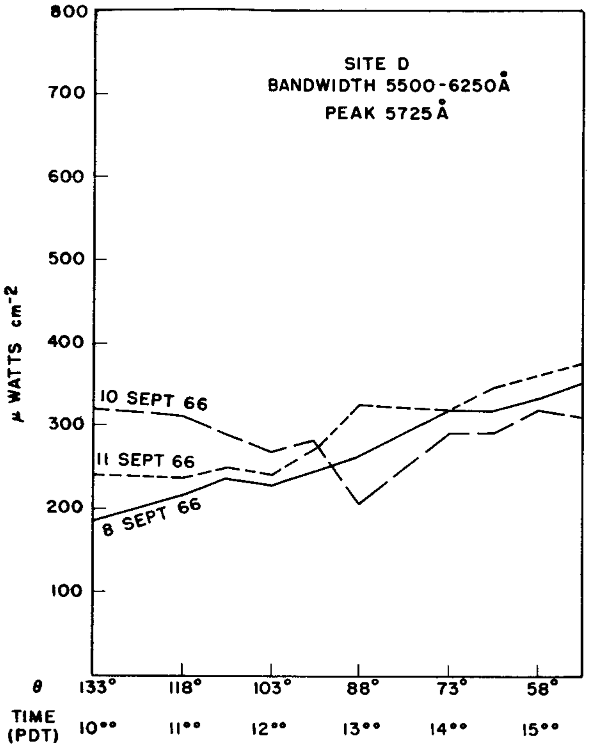
SITE D
BANDWIDTH 5500-6250Å
PEAK 5725Å
800
700
600
500
400
300
200
100
μ WATTS cm⁻²
10 SEPT 66
11 SEPT 66
8 SEPT 66
θ
133°
118°
103°
88°
73°
58°
TIME (PDT)
10⁰⁰
11⁰⁰
12⁰⁰
13⁰⁰
14⁰⁰
15⁰⁰

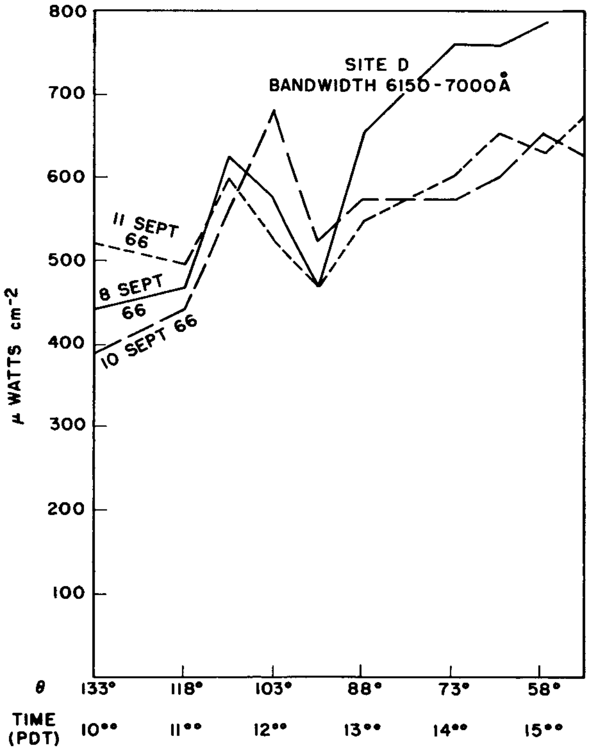
SITE D
BANDWIDTH 6150-7000Å
800
700
600
500
400
300
200
100
μ WATTS cm⁻²
11 SEPT 66
8 SEPT 66
10 SEPT 66
θ
133°
118°
103°
88°
73°
58°
TIME (PDT)
10⁰⁰
11⁰⁰
12⁰⁰
13⁰⁰
14⁰⁰
15⁰⁰

Unclassified

Security Classification

14. KEY WORDS	LINK A		LINK B		LINK C	
	ROLE	WT	ROLE	WT	ROLE	WT
Multispectral Photography						
Geology						
Photometry						

INSTRUCTIONS

1. ORIGINATING ACTIVITY: Enter the name and address of the contractor, subcontractor, grantee, Department of Defense activity or other organization *(corporate author)* issuing the report.

2*a*. REPORT SECURITY CLASSIFICATION: Enter the overall security classification of the report. Indicate whether "Restricted Data" is included. Marking is to be in accordance with appropriate security regulations.

2*b*. GROUP: Automatic downgrading is specified in DoD Directive 5200.10 and Armed Forces Industrial Manual. Enter the group number. Also, when applicable, show that optional markings have been used for Group 3 and Group 4 as authorized.

3. REPORT TITLE: Enter the complete report title in all capital letters. Titles in all cases should be unclassified. If a meaningful title cannot be selected without classification, show title classification in all capitals in parenthesis immediately following the title.

4. DESCRIPTIVE NOTES: If appropriate, enter the type of report, e.g., interim, progress, summary, annual, or final. Give the inclusive dates when a specific reporting period is covered.

5. AUTHOR(S): Enter the name(s) of author(s) as shown on or in the report. Enter last name, first name, middle initial. If military, show rank and branch of service. The name of the principal author is an absolute minimum requirement.

6. REPORT DATE: Enter the date of the report as day, month, year, or month, year. If more than one date appears on the report, use date of publication.

7*a*. TOTAL NUMBER OF PAGES: The total page count should follow normal pagination procedures, i.e., enter the number of pages containing information.

7*b*. NUMBER OF REFERENCES: Enter the total number of references cited in the report.

8*a*. CONTRACT OR GRANT NUMBER: If appropriate, enter the applicable number of the contract or grant under which the report was written.

8*b*, 8*c*, & 8*d*. PROJECT NUMBER: Enter the appropriate military department identification, such as project number, subproject number, system numbers, task number, etc.

9*a*. ORIGINATOR'S REPORT NUMBER(S): Enter the official report number by which the document will be identified and controlled by the originating activity. This number must be unique to this report.

9*b*. OTHER REPORT NUMBER(S): If the report has been assigned any other report numbers *(either by the originator or by the sponsor)*, also enter this number(s).

10. AVAILABILITY/LIMITATION NOTICES: Enter any limitations on further dissemination of the report, other than those imposed by security classification, using standard statements such as:

(1) "Qualified requesters may obtain copies of this report from DDC."

(2) "Foreign announcement and dissemination of this report by DDC is not authorized."

(3) "U. S. Government agencies may obtain copies of this report directly from DDC. Other qualified DDC users shall request through ________________."

(4) "U. S. military agencies may obtain copies of this report directly from DDC. Other qualified users shall request through ________________."

(5) "All distribution of this report is controlled. Qualified DDC users shall request through ________________."

If the report has been furnished to the Office of Technical Services, Department of Commerce, for sale to the public, indicate this fact and enter the price, if known.

11. SUPPLEMENTARY NOTES: Use for additional explanatory notes.

12. SPONSORING MILITARY ACTIVITY: Enter the name of the departmental project office or laboratory sponsoring *(paying for)* the research and development. Include address.

13. ABSTRACT: Enter an abstract giving a brief and factual summary of the document indicative of the report, even though it may also appear elsewhere in the body of the technical report. If additional space is required, a continuation sheet shall be attached.

It is highly desirable that the abstract of classified reports be unclassified. Each paragraph of the abstract shall end with an indication of the military security classification of the information in the paragraph, represented as *(TS)*, *(S)*, *(C)*, or *(U)*.

There is no limitation on the length of the abstract. However, the suggested length is from 150 to 225 words.

14. KEY WORDS: Key words are technically meaningful terms or short phrases that characterize a report and may be used as index entries for cataloging the report. Key words must be selected so that no security classification is required. Identifiers, such as equipment model designation, trade name, military project code name, geographic location, may be used as key words but will be followed by an indication of technical context. The assignment of links, rules, and weights is optional.

Unclassified

Security Classification

Unclassified
Security Classification

DOCUMENT CONTROL DATA - R&D		
(Security classification of title, body of abstract and indexing annotation must be entered when the overall report is classified)		
1. ORIGINATING ACTIVITY *(Corporate author)* Hq AFCRL, OAR (CRJ) United States Air Force Bedford, Massachusetts 01730	2a. REPORT SECURITY CLASSIFICATION Unclassified 2b. GROUP	
3. REPORT TITLE Terrestrial Multispectral Photography		
4. DESCRIPTIVE NOTES *(Type of report and inclusive dates)* Scientific Report. Final, 1 October 1966.		
5. AUTHOR(S) *(Last name, first name, initial)* CRONIN, J. F.		
6. REPORT DATE January 1967	7a. TOTAL NO. OF PAGES 46	7b. NO. OF REFS 15
8a. CONTRACT OR GRANT NO. Partially supported under NASA DPR No. R22-13-012 fund transfer b. PROJECT AND TASK NO. 7628-05 c. DOD ELEMENT 62405394 d. DOD SUBELEMENT 681000	9a. ORIGINATOR'S REPORT NUMBER(S) AFCRL-67-0076 Special Reports No. 56 9b. OTHER REPORT NO(S) *(Any other numbers that may be assigned this report)* AFCRL-67-0076	
10. AVAILABILITY/LIMITATION NOTICES Distribution of this document is unlimited.		
11. SUPPLEMENTARY NOTES	12. SPONSORING MILITARY ACTIVITY Hq AFCRL, OAR (CRJ) United States Air Force Bedford, Massachusetts 01730	

13. ABSTRACT

Remote multispectral photographic sensing of the earth's surface may be a feasible means of identifying and discriminating between inorganic terrestrial materials differing in composition or physical characteristics. Simultaneous airborne and ground-based photographic and photometric studies of such sites as Mono Craters, California, indicate that within the range of the photographic spectrum (2900 Å to 14000 Å), the most promising region for the geologist and other earth scientists could be the wavelengths outside the visible spectrum.

DD FORM 1 JAN 64 1473

Unclassified
Security Classification